Neurobiology of Disease 54 (2013) 32–42

Contents lists available at SciVerse ScienceDirect

Neurobiology of Disease

journal homepage: www.elsevier.com/locate/ynbdi

PACAP signaling exerts opposing effects on neuroprotection and neuroinflammation during disease progression in the SOD1(G93A) mouse model of amyotrophic lateral sclerosis ☆

Cornelia Ringer [a], Luisa-Sybille Büning [a], Martin K.H. Schäfer [a], Lee E. Eiden [b], Eberhard Weihe [a,*], Burkhard Schütz [a,*]

[a] Institute of Anatomy and Cell Biology, Philipps-University, Marburg, Germany
[b] Laboratory on Cellular and Molecular Regulation, National Institute of Mental Health, National Institutes of Health, Bethesda, MD, USA

ARTICLE INFO

Article history:
Received 8 September 2012
Revised 8 February 2013
Accepted 22 February 2013
Available online 4 March 2013

Keywords:
Amyotrophic lateral sclerosis
Microglia
Neuroinflammation
Neuroprotection
Neuropeptide
Parasympathetic
Sympathetic

ABSTRACT

Pituitary adenylate cyclase-activating polypeptide (PACAP) is a pleiotropic peptide with autocrine neuroprotective and paracrine anti-inflammatory properties in various models of acute neuronal damage and neurodegenerative diseases. Therefore, we examined a possible beneficial role of endogenous PACAP in the superoxide dismutase 1, SOD1(G93A), mouse model of amyotrophic lateral sclerosis (ALS), a lethal neurodegenerative disease particularly affecting somatomotor neurons. In wild-type mice, somatomotor and visceromotor neurons in brain stem and spinal cord were found to express the PACAP specific receptor PAC1, but only visceromotor neurons expressed PACAP as a potential autocrine source of regulation of these receptors. In SOD1(G93A) mice, only a small subset of the surviving somatomotor neurons showed induction of PACAP mRNA, and somatomotor neuron degeneration was unchanged in PACAP-deficient SOD1(G93A) mice. Pre-ganglionic sympathetic visceromotor neurons were found to be resistant in SOD1(G93A) mice, while pre-ganglionic parasympathetic neurons degenerated during ALS disease progression in this mouse model. PACAP-deficient SOD1(G93A) mice showed even greater pre-ganglionic parasympathetic neuron loss compared to SOD1(G93A) mice, and additional degeneration of pre-ganglionic sympathetic neurons. Thus, constitutive expression of PACAP and PAC1 may confer neuroprotection to central visceromotor neurons in SOD1(G93A) mice via autocrine pathways. Regarding the progression of neuroinflammation, the switch from amoeboid to hypertrophic microglial phenotype observed in SOD1(G93A) mice was absent in PACAP-deficient SOD1(G93A) mice. Thus, endogenous PACAP may promote microglial cytodestructive functions thought to drive ALS disease progression. This hypothesis was consistent with prolongation of life expectancy and preserved tongue motor function in PACAP-deficient SOD1(G93A) mice, compared to SOD1(G93A) mice. Given the protective role of PACAP expression in visceromotor neurons and the opposing effect on microglial function in SOD1(G93A) mice, both PACAP agonism and antagonism may be promising therapeutic tools for ALS treatment, if stage of disease progression and targeting the specific auto- and paracrine signaling pathways are carefully considered.

Introduction

Pituitary adenylate cyclase-activating polypeptide (PACAP), initially isolated from the hypothalamus (Miyata et al., 1989), is a member of the vasoactive intestinal polypeptide (VIP)/secretin/glucagon superfamily. Two biologically active PACAP isoforms of different length exist, PACAP-38 and the C-terminally truncated PACAP-27 (Miyata et al., 1989, 1990), with PACAP-38 being the predominant form (Arimura et al., 1991). PACAP is found in numerous areas and neuron types throughout the central and peripheral nervous system, e.g. in hippocampus, amygdala, substantia nigra, cerebellar granule cells and sensory neurons in the dorsal root ganglia, as well as sympathetic, parasympathetic and some somatomotor neurons (reviewed by Hannibal, 2002; Fahrenkrug and Hannibal, 2004). PACAP acts in an autocrine and paracrine manner through activation of three G-protein-coupled transmembrane receptors. PAC1 is the PACAP-specific receptor predominantly expressed in brain and adrenal chromaffin cells. VPAC1 and VPAC2 bind PACAP and the related neuropeptide VIP with similar affinities and are expressed by various cell types including neurons, glia cells, endothelial cells, lymphocytes and

Abbreviations: ALS, amyotrophic lateral sclerosis; PACAP, pituitary adenylate cyclase-activating polypeptide; PAC1, PACAP receptor 1; SOD1, superoxide dismutase 1.

☆ The work described has been carried out in accordance with Uniform Requirements for manuscripts submitted to biomedical journals.

* Corresponding authors at: Molecular Neurosciences Department, Institute of Anatomy and Cell Biology, University of Marburg, Robert-Koch-Strasse 8, 35037 Marburg, Germany. Fax: +49 6421 2868965.
E-mail addresses: weihe@staff.uni-marburg.de (E. Weihe), schuetzb@staff.uni-marburg.de (B. Schütz).

Available online on ScienceDirect (www.sciencedirect.com).

0969-9961/$ – see front matter © 2013 Elsevier Inc. All rights reserved.
http://dx.doi.org/10.1016/j.nbd.2013.02.010

macrophages (Dickson and Finlayson, 2009; Laburthe et al., 2007). Accordingly, PACAP is involved in multiple physiological functions such as brain development, circadian rhythm, stress response and inflammation (reviewed in Delgado et al., 2003; Mertens et al., 2007; Seaborn et al., 2011; Stroth et al., 2011).

Endogenous PACAP, as well as exogenously applied PACAP, have been shown to be neuroprotective in several pathophysiological contexts. PACAP reduced infarct volume following ischemia (Chen et al., 2006; Ohtaki et al., 2006; Reglodi et al., 2002) and neuronal loss after traumatic damage of spinal cord (Chen and Tzeng, 2005). In models of facial and spinal axotomy, PACAP was found up-regulated in sensory, motor and sympathetic neurons (Armstrong et al., 2003; Moller et al., 1997; Pettersson et al., 2004; Zhang et al., 1996; Zhou et al., 1999), and the depletion of PACAP resulted in an enhanced microglia reaction and delayed axon re-growth (Armstrong et al., 2008). PACAP-deficient mice showed symptom exacerbation in an experimental autoimmune encephalomyelitis mouse model of multiple sclerosis (Tan et al., 2009). Long term intranasal application of PACAP increased cognitive functions and survival in a mouse model of Alzheimer's disease (Rat et al., 2011), and intravenous application of PACAP ameliorated motor function in two mouse models of Parkinson's disease (Reglodi et al., 2004, 2006; Wang et al., 2008).

According to in vivo studies and a plethora of experiments on different neuronal and glial cell types in cell culture, it has been suggested that PACAP mediates its neuroprotective effects via both direct autocrine anti-apoptotic pathways on neurons and indirect paracrine, anti-inflammatory mechanisms via glial cell signaling (reviewed by Dejda et al., 2005, 2011; Leceta et al., 2000; Shioda et al., 2006).

The effects of PACAP in amyotrophic lateral sclerosis (ALS), an invariably fatal neurodegenerative disease characterized by the progressive loss of upper (cortex) and lower (brain stem and spinal cord) somatomotor neurons, are not known. Clinically, the propagating degeneration of somatomotor neurons with denervation of skeletal muscles results in paralysis leading to death by respiratory failure approximately 3–5 years after disease onset (Kiernan et al., 2011; Rothstein, 2009). While 90% of all ALS cases occur spontaneously (sporadic ALS), 10% are inherited (familial ALS) with 2% among these caused by mutations in the gene encoding superoxide dismutase 1 (SOD1, (Rosen et al., 1993)). The disease causing the G93A variant of human SOD1 is recapitulated in a transgenic mouse line that develops disease signs comparable to human ALS (Gurney et al., 1994). Despite extensive research on ALS patients and the SOD1(G93A) mouse model, the molecular mechanisms underlying motor neuron degeneration are still not well understood. Besides intracellular events, e.g. oxidative stress, and dysfunction of mitochondria and protein aggregation (Kiernan et al., 2011; Rothstein, 2009), glutamate-induced excitotoxicity (Bogaert et al., 2010) and recently glial cell actions have been implicated in the onset and progression of SOD1-associated ALS (Clement et al., 2003; Ilieva et al., 2009; Papadeas et al., 2011).

The finding that PACAP is induced by motor neurons in neuronal injury models (Armstrong et al., 2003; Chen and Tzeng, 2005; Mesnard et al., 2011) and was able to protect rat motor neurons in culture against glutamate-induced excitotoxicity (Tomimatsu and Arakawa, 2008) prompted us to investigate the role of PACAP in affecting disease progression in the SOD1(G93A) mouse model of ALS. We analyzed PACAP and PACAP receptor mRNA expression in motor neurons in wild-type compared to SOD1(G93A) mice to establish the chemical neuroanatomy underlying PACAP signaling in ALS, and then crossbred PACAP-deficient (Hamelink et al., 2002) and SOD1(G93A) transgenic mice, to determine the in vivo effect of PACAP depletion on the pathogenesis of ALS.

Material and methods

Animals

Transgenic mice of the strain B6SJL-TgN(SOD1(G93A))1Gur (The Jackson Laboratory, Bar Harbor, ME), which hemizygously carry human SOD1(G93A) with the pathogenic G93A mutation in high copy number (Gurney et al., 1994), were used. Progeny for experimental analysis were obtained from breeding pairs between SOD1(G93A) males and C57BL/6 wild-type females. Littermates were either carriers of the transgene or wild-type. Mice with a targeted loss-of-function mutation of the PACAP gene (Hamelink et al., 2002), and bred to 12 generations on a C57Bl/6N background were used in these studies. SOD1(G93A) and PACAP-deficient mice were identified by PCR with established primers and protocols (Hamelink et al., 2002; Schütz et al., 2005), using genomic DNA obtained from ear biopsies. All mice were housed in groups of two to four animals per cage on a 12 h dark/light cycle with unrestricted access to food and water. From the time mice carrying the SOD1(G93A) mutation showed motor deficits, additional moisturized food and water were placed on the cage floor. Because of ethical considerations, transgenic animals were killed when their weight dropped below 80% of peak body weight. All animal procedures were conducted in accordance with EU Directive 2010/63/EU for animal experiments, and according to the German Animal Protection Law under a protocol approved by the county administrative government in Gießen, and adequate measures were taken to minimize pain or discomfort. To obtain double transgenic mice, PACAP-deficient females were mated with SOD1(G93A) males. Within the offspring, PACAP-hemizygous females were mated with SOD1(G93A):PACAP-hemizygeous males, which resulted in the generation of six genotypes in the expected Mendelian frequency, from which four genotypes were used for experimental analysis: wild-type (=WT), PACAP-deficient (=PACAP−/−), SOD1(G93A) (=SOD1), and PACAP-deficient SOD1(G93A) (=SOD1:PACAP−/−). The group names defined here will be used throughout the report even in those cases where tissue was analyzed that was derived from the parental single-transgenic mouse colonies. In each group, roughly equal numbers of female and male mice were used.

Motor functions and disease progression

The motor performances of all mice were assessed weekly with the paw grip endurance test targeting hind limb function (Schütz et al., 2005), and a licking test targeting tongue motor function (Fuchs et al., 2010; Hayar et al., 2006). For testing paw grip endurance, the mice were placed individually on a meshed wire platform at a height of about 60 cm above the bench. After the animal found a grip, the platform was gently turned upside-down and the latency recorded until the animal let loose with both hind legs or succeeded to reach the 120 s cutoff time. Each mouse was given a maximum of three consecutive trials to reach the cut-off, and the longest latency was recorded. Motor function of the tongue was determined recording the licking frequency during drinking. Mice were placed in a cage equipped with a metal floor and water bottle with a metal spout, both connected to an analog/digital converter. Each lick of the mouse closed the current circuit, thereby inducing a minimal, non-perceptible voltage. These peaks were recorded by the converter and conferred on a computer. Time differences between 25 consecutive voltage peaks (=tongue licks) were averaged and calculated as lick frequency in hertz (Hz). As additional parameters for disease progression, body weight and survival time were monitored. Body weight was determined weekly and expressed as percentage of the weight at the beginning of the study period (P49) to account for absolute weight differences between individual mice. From the time mice showed severe motor symptoms, body weight was determined daily. All clinical parameters were subjected to statistical analysis (see below).

Tissue processing

Mice were killed by exposure to an overdose of inhaled isoflurane. Lumbar and thoracic segments of spinal cord, and brains were quickly dissected and either directly frozen in −40 °C cold isopentane, or immersion-fixed for 48 h in Bouin Hollande fixative, containing 4%

(w/v) picric acid, 2.5% (w/v) cupric acetate, 3.7% (v/v) formaldehyde, and 1% (v/v) glacial acetic acid. Following Bouin Hollande fixation, the tissues were extensively washed in 70% isopropanol, dehydrated, cleared with xylene, and embedded in paraffin. Seven micrometer thick sections were cut with a microtome and mounted onto silanized glass slides. Histological counter stains were done with Giemsa stain.

In situ hybridization

Complementary RNA probes for the specific detection of mouse PACAP, PAC1, VPAC1, and VPAC2 transcripts in tissue sections were generated by PCR from mouse C57Bl/6 spinal cord cDNA (see Table 1 for details) and subcloned into pGEM-T (Promega, Heidelberg, Germany). Gene-specific riboprobes were generated using T7 and Sp6 RNA polymerase for antisense and sense probe, respectively, depending on insert orientation. The specificity of the PACAP riboprobe could be confirmed by the absence of specific ISH signals in spinal cord sections taken from PACAP−/− mice. The VAChT riboprobe (NM_021712, bp 1021–1775) used for the specific labeling of motor neurons was described previously (Fuchs et al., 2010; Ringer et al., 2012).

For the detection of two different RNA transcripts on the same tissue section a digoxigenin (Dig)-labeled VAChT riboprobe was generated by in vitro transcription with a Dig-labeling mix containing 10 mmol/l each of ATP, CTP, and GTP; 6.5 mmol/l UTP; and 3.5 mmol/l Dig-11-UTP (Roche, Basel, Switzerland). The VAChT-Dig riboprobe was added at a concentration of 2 ng/μl to the ^{35}S-labeled PACAP, PAC1, VPAC1, or VPAC2 hybridization mixes. Hybridization and post-hybridization washes of 14 μm thick tissue sections were performed as described in detail earlier (Fuchs et al., 2010). The detection of Dig-conjugated VAChT probes was performed with alkaline phosphatase-conjugated anti-DIG antibodies diluted to 1 unit/ml and 0.2 mM 5-bromo-4-chloro-3-indolyl phosphate and nitroblue tetrazolium salt (Roche, Mannheim, Germany) yielding a blue precipitate after 16 h. For the subsequent detection of the ^{35}S-labeled riboprobes, slides were covered with K5 photoemulsion (Ilford, Marly, Switzerland) diluted to 1:1 in water. After exposure for 21 days in the dark at 4 °C, slides were developed, extensively washed in tap water, and embedded with 42 °C warm gelatin embedding medium. Bright and dark field microscopic analysis was performed using an Olympus AX70 microscope (Olympus Optical, Hamburg, Germany).

Immunohistochemistry

Sections on glass slides were deparaffinized in xylene and rehydrated through a graded series of isopropanol. Endogenous peroxidase activity was blocked by incubation in methanol/0.3% H_2O_2 for 30 min and antigen retrieval achieved by incubation in 10 mM sodium citrate buffer (pH 6.0) at 92–95 °C for 15 min. Nonspecific binding sites were blocked with 5% bovine serum albumin (BSA) in 50 mM phosphate buffered saline (PBS, pH 7.45) for 30 min, followed by an avidin–biotin blocking step (Avidin–Biotin Blocking Kit, Boehringer, Ingelheim, Germany) for 40 min. Primary antibodies (goat-anti-choline-acetyltransferase, 1:500, Chemicon, Hofheim, Germany; guinea pig-anti-glial fibrillary acidic protein, 1:5000, Progen, Heidelberg, Germany; rabbit-anti-ionized calcium binding adaptor molecule 1, 1:2500, Wako Chemicals, Neuss, Germany; rabbit-anti-Cluster of differentiation 3, 1:3000, DAKO, Hamburg, Germany; rabbit anti-PACAP38, 1:20,000, Progen, Heidelberg, Germany) were applied in PBS/1% BSA and incubated at 16 °C overnight followed by 2 h at 37 °C. After several washes in distilled water followed by rinsing in PBS, the sections were incubated for 45 min at 37 °C with species-specific biotinylated secondary antibodies (Dianova, Hamburg, Germany), diluted to 1:200 in PBS/1% BSA, washed again several times and incubated for 30 min with avidin–biotin–peroxidase complex reagents (Vectastain Elite ABC kit; Vector Laboratories, Burlingame, CA). Immunoreactions were visualized by 8 min incubation with 3,3-diaminobenzidine (DAB, Sigma Aldrich, Deisenhofen, Germany), enhanced by the addition of 0.08% ammonium nickel sulfate (Fluka, Bucks, Switzerland), which resulted in a dark blue staining. After three 5 min washes in distilled water, the sections were dehydrated through a graded series of isopropanol, cleared in xylene and finally mounted under coverslips. Digital bright-field pictures were taken with an Olympus AX70 microscope (Olympus Optical, Hamburg, Germany), equipped with a SPOT RT Slider Camera and SPOT image analysis software (Version 3.4; Diagnostic Instruments Inc., Seoul, Korea).

Densitometry and neuron counts

For a quantitative analysis of immunoreactivities, images from bright-field IHC staining were acquired with MCID Elite™ 7.0 software (Imaging Research Inc., St. Catherines, Canada) and analyzed with ImageJ (National Institutes of Health, Bethesda, Maryland, USA). For astrocyte, microglia and lymphocyte quantification, immunoreactive structures were determined by setting a constant threshold of optic density in the area of interest, i.e. the lateral aspect of the ventral horn grey matter (Kong and Xu, 1998) and the para-medial brain stem, respectively. All immunoreactions above threshold were gathered and given as percentage immunoreactive area for astrocytes and microglia as number of immunoreactive particles (at least 20 connected pixels) per area for lymphocytes, respectively. Motor neurons were counted manually, including only soma with clearly cut and healthy looking (round) nucleus to exclude neurons in degeneration. In addition, multiple sections from a single tissue were 21 μm apart to avoid double counting of neurons.

Table 1
Selection of PCR primer pairs for the generation of gene-specific riboprobes for in situ hybridization experiments.

Name	Gene	*e*!Ensembl	Primer	Amplicon length (bp)
PACAP	Adcyap1	ENSMUSG00000024256	Forward: TTACGACCAGGACGGAAACC Reverse: AACAGCTCAGGCGAATTTTCA	701
PAC1	Adcyap1r1, transcript variant 1	ENSMUSG00000029778	Forward: CCTATGGCTATTGCTATGCACTC reverse: AGAGTAATGGTGGATAGTTCTGACA	1085
VPAC1	Vipr1	ENSMUSG00000032528	Forward: GGTGGCCATCCTCTACTGCTTC reverse: CCTCCCCAGGCTTTTATGTCAG	1172
VPAC2	Vipr2	ENSMUSG00000011171	Forward: AGTGCTGCTGGGTTTGACATA reverse: ATAGGCTGTGCCAGAACACTAGG	985

bp = base pair.

Statistical analysis

All values are presented as mean and standard error of the mean (SEM). A Kaplan–Meier curve of survival analysis was analyzed with a Logrank test. All other data were first analyzed for Gaussian distribution and the differences between groups in motor tests and body weight examined for statistical significance using two-way ANOVA followed by Bonferroni post hoc testing. The last data values of mice that died before the end of the experiment were carried forward. Motor neuron counts and densitometric analyses of inflammatory cells were analyzed by one-way ANOVA followed by Bonferroni post-hoc test. For the additional comparison of two groups, the *t*-test was applied. *p* values less than 0.05 were regarded as significant.

Results

Somato- and visceromotor nuclei of wild-type mice express different PACAP ligand-receptor combinations

Since autocrine and paracrine effects of PACAP on motoneurons and glia, respectively, may depend on the spatial co-expression of ligand and receptor, we first determined the presence of PACAP, PAC1, VPAC1 and VPAC2 mRNA in motoneuron nuclei of WT mice by double in situ hybridization histochemistry. We used para-median sections through the caudal brain medulla, where the visceromotor (parasympathetic) dorsal vagal nucleus (X) directly adjoins the somatomotor hypoglossal nucleus (XII, Fig. 1A). A digoxygenin-labeled VAChT riboprobe was used to label all motor neurons, and combined individually with radioactively-labeled PACAP or PACAP receptor riboprobes. Strong PACAP mRNA expression was detected in all X neurons, as expected (Hannibal, 2002), but was undetectable in XII neurons (Fig. 1B) and glia. Weak PAC1 mRNA signals were scattered over all X and XII neuronal profiles (Fig. 1C), while VPAC1 messages were concentrated in spots outside motor neuron profiles, suggesting expression in glia (Fig. 1D). Finally, VPAC2 mRNA was present in XII neurons and glia, but was undetectable in X neurons (Fig. 1E). Identical expression patterns were found in other somatomotor and parasympathetic motor nuclei in brain stem as well as somatomotor and sympathetic motoneurons in the ventral horn and lateral horn of lumbar and thoracic spinal cord, respectively (data not shown). Hence, autocrine effects of PACAP in vivo may be most relevant for central autonomic neurons, while paracrine effects on glia may be uniformly relevant throughout the motor system.

Single somatomotor neurons induce PACAP expression during ALS disease progression

Since PACAP has been found transcriptionally up-regulated in many facial somatomotor neurons in response to axotomy in pre-symptomatic (P70) SOD1 mice (Mesnard et al., 2011), we hypothesized that such mechanism also occurs during the regular course of chronic neurodegeneration in the SOD1-based ALS disease model. Again, double in situ hybridization histochemistry with VAChT and PACAP was performed on para-median brain stem sections of SOD1 mice at a pre-symptomatic age (P40) and at disease end-stage. At P40, PACAP mRNA expression was undetectable in somatomotor neurons of XII (Figs. 2A + B) and VII (Figs. 2E + F), but at high levels in parasympathetic neurons of X (Fig. 2B), equivalent to WT (compare to Fig. 1). At disease end-stage, PACAP expression in X remained unchanged, while in XII (Figs. 2C + D) and VII (Figs. 2G + H) a few single neurons were found to have induced PACAP expression (arrows in Figs. 2D + F). However, the majority of the surviving somatomotor neurons still did not display PACAP mRNA. PACAP mRNA induction pattern was also exiguous in somatomotor neurons in the lumbar spinal cord. In all investigated somatomotor areas the minor to negligible response patterns of PACAP to SOD1 mutation were also seen on the protein level (immunohistochemical data provided as supplemental figures). Thus, an ALS-associated general induction of PACAP in somatomotor neurons does not occur.

PACAP protects against pre-ganglionic visceromotor, but not somatomotor neuron loss during ALS disease progression

In a previous study (Fuchs et al., 2010) we had observed that neuropathological disease signs were not restricted to areas with somatomotor neurons, i.e. the hypoglossal nucleus, but also present in a visceromotor nucleus, i.e. the parasympathetic dorsal nucleus of the vagus nerve. Moreover, since PACAP and PAC1 were found ubiquitously co-expressed by autonomic neurons (this report and Hamelink et al., 2002), we first characterized in detail disease-related changes in both visceromotor parasympathetic and sympathetic areas.

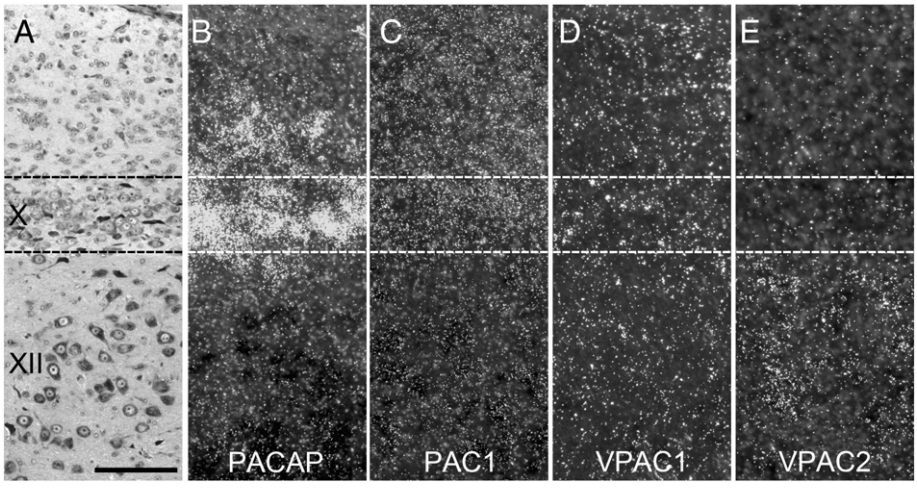

Fig. 1. PACAP ligand-receptor systems in wild-type (WT) somatomotor and visceromotor nuclei. (A) Giemsa-stained paramedian section through the caudal brain medulla. X = dorsal nucleus of the vagus nerve (visceromotor) and XII = hypoglossal nucleus (somatomotor). (B–E) Dark-field images from double in situ hybridization histochemistry to simultaneously detect VAChT mRNA (digoxygenin-label, black signals) in combination with PACAP, PAC1, VPAC1, and VPAC2 mRNA (radioactive-label, white dots), respectively. Note the presence of PACAP transcripts in visceromotor neurons, PAC1 in viscero- and somatomotor neurons, VPAC1 in glial cells within these nuclei but absence from both motor neuron pools, and VPAC2 in somatomotor, but not visceromotor neurons. Scale bar in (A) equals 100 μm and accounts for all panels.

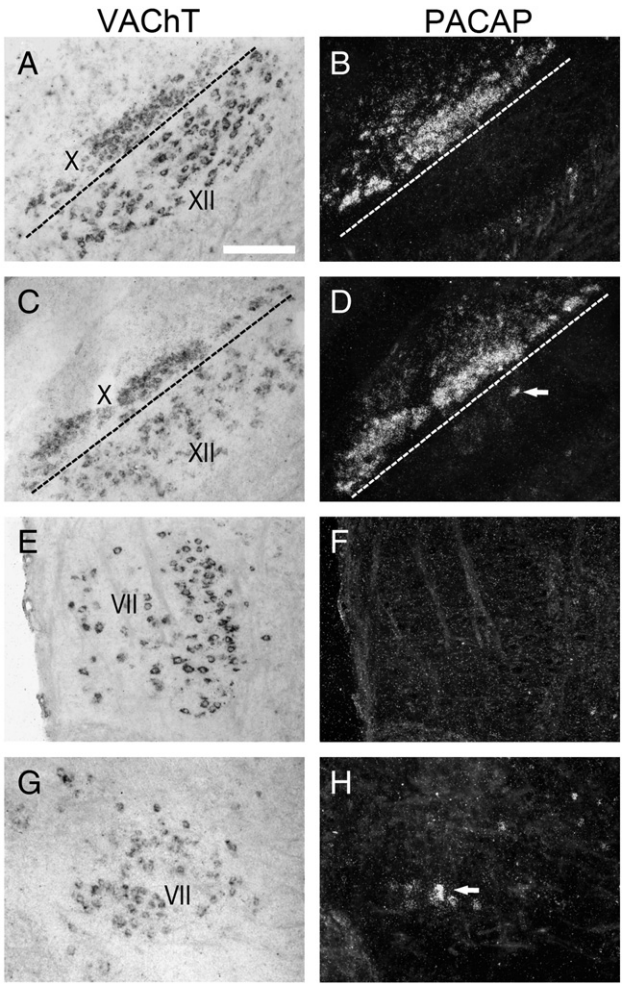

Fig. 2. Induction of PACAP mRNA in single somatomotor neurons at end-stage in SOD1 mice. Double in situ hybridization histochemistry for VAChT mRNA (Digoxigenin-labeled riboprobe, left panels) and PACAP mRNA (radioactive-labeled riboprobe, right panels) on the same section. VAChT labels all somatomotor (facial, VII; hypoglossal, XII) and visceromotor (vagal, X) neurons. At P40 (A, B + E, F), somatomotor neurons in the hypoglossal (XII) and facial (VII) nucleus did not express PACAP (B + F), while all visceromotor neurons of the vagal nucleus (X) displayed uniform PACAP mRNA expression (B). In end-stage SOD1 mice (C, D + G, H), PACAP-expression in X apparently was unchanged (D), and only a few of the remaining somatomotor neurons (arrows) had induced PACAP expression in both XII (D) and VII (H). Scale bar in (A) equals 200 μm and accounts for all panels.

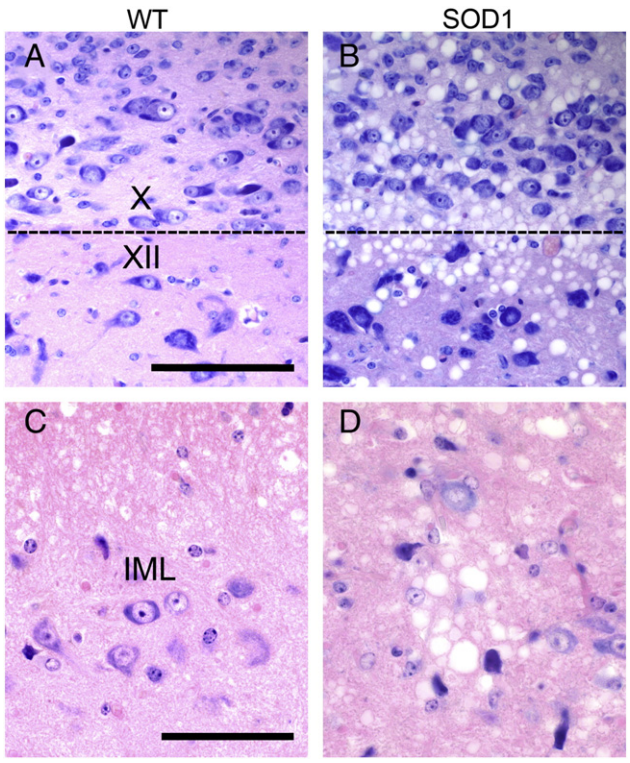

Fig. 3. Neuropathology of the pre-ganglionic parasympathetic and sympathetic systems in SOD1 mice. (A + B) Giemsa-stained para-median sections through the vagal (X) and hypoglossal (XII) nuclei from P120 WT and end-stage SOD1 mice. The dashed lines indicate the border between the two nuclei. Note vacuolization in the neuropil of end-stage SOD1 mice (B) that is present in both nuclei. (C + D) Giemsa-stained transverse sections of the intermediolateral cell column (IML) in the thoracic spinal cord. In P120 WT mice (C), groups of IML neurons are separated by dense and uniform neuropil. In SOD1 mice at disease end-stage (D), the IML center is characterized by presence of pathologic vacuoles, which have displaced the IML neurons. Scale bar in (A) equals 100 μm and accounts for pictures A + B; scale bar in (C) equals 50 μm and accounts for C + D.

On Giemsa-stained para-median brain stem sections from P120 WT mice (Fig. 3A), X and XII neurons were found embedded in a homogenous neuropil. In end-stage SOD1 mice, pathology-related vacuoles were present in both nuclei, but most frequently located at the border between the two nuclei (Fig. 3B). Sympathetic pre-ganglionic visceromotor neurons are organized in a bilateral inter-connected chain in the intermediolateral cell column (IML) of the thoracic and upper lumbar spinal cord (Llewellyn-Smith, 2009). While in P120 WT mice (Fig. 3C), IML neuronal cell bodies were surrounded by a homogenous neuropil, a massive vacuolar pathology with displacement of IML neurons was present at end-stage in SOD1 mice (Fig. 3D). In the central compartments of the autonomic nervous system (ANS), vacuolar pathology appeared around P90, i.e. at disease onset, and was confined to neurites (data not shown). The observed neuropathology of the autonomic visceromotor nervous system in SOD1 mice was restricted to the central pre-ganglionic division. Post-ganglionic neurons and fibers in the periphery, e.g. in the mandibular glands (parasympathetic) or the stellate ganglion (sympathetic), respectively, were morphologically unaffected (data not shown).

To investigate if the observed neuropathology in the ANS of SOD1 mice was accompanied by neuron loss, or if these neurons instead were protected due to the presence of PACAP (and PAC1), we crossed a PACAP-deficient mouse strain (Hamelink et al., 2002) into the SOD1 ALS mouse model and determined motoneuron numbers, as well as clinical outcome and survival of PACAP−/− SOD1 mice (=SOD1:PACAP−/−) in comparison to PACAP+/+ SOD1 littermates (=SOD1) and their respective WT groups (WT for SOD1 and PACAP−/− for SOD1:PACAP−/−). Tissue sections from end-stage SOD1 mice and age matched (P120) control mice containing the X and XII nuclei, and sections from thoracic spinal cord were immunohistochemically stained for ChAT, and assessed qualitatively and quantitatively. In WT and PACAP−/−, ChAT immunostaining in X and XII labeled motoneuron cell bodies and neurites (Figs. 4A + B). In both SOD1 groups, morphologies of X and XII motoneuron somata were mostly unaffected by the disease (Figs. 4C + D), while all pathology-related vacuoles in the neuropil were lined by ChAT-immunoreactivity and therefore were most likely of motor neuron origin, e.g. neurits. In addition, a few parasympathetic motoneurons in X of SOD1:PACAP−/− animals had vacuoles in their soma (Fig. 4D).

Until end-stage, SOD1 and SOD1:PACAP−/− mice had lost about 40% of XII neurons when compared to their respective WT group (Fig. 4I), with final XII neuron loss similar in both SOD1 genotypes (WT = 55.3 ± 4.6 vs. SOD1 = 34.5 ± 4.6, and PACAP−/− = 54.5 ± 5.3 vs. SOD1:PACAP−/− = 35.7 ± 2.9, all N = 4, $n = 6$). In the lumbar ventral horn, motoneuron degeneration also occurred without differences between the two PACAP genotypes (WT = 7.0 ± 1.4 vs. SOD1 = 2.7 ± 1.3, and PACAP−/− = 6.8 ± 1.3 vs.

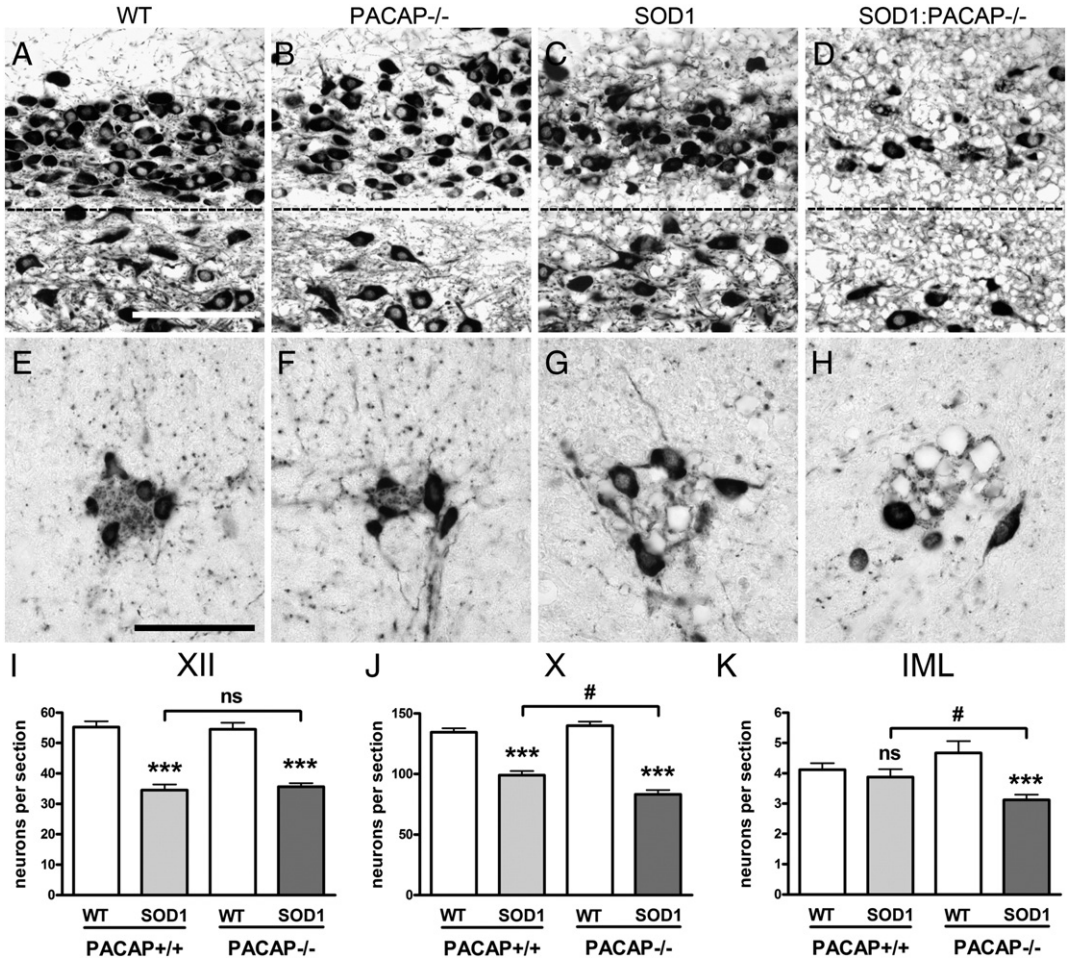

Fig. 4. Somatomotor and visceromotor neurodegeneration in SOD1 and SOD1:PACAP−/− mice. (A–H) ChAT immunolabeling of the vagal/hypoglossal nuclei (upper panel) and of the IML (lower panel) from end-stage mice. Note ChAT-immunoreactivity surrounding pathologic vacuoles in SOD1-harboring genotypes. Scale bar in (A) equals 100 μm and accounts for pictures (A–D); scale bar in (E) equals 50 μm and accounts for (E–H). (I–K) Quantification of somatomotor hypoglossal (XII), parasympathetic vagal (X) and sympathetic (IML) neurons based on ChAT-immunoreactivities. ***$p < 0.001$ SOD1 compared to respective WT (WT or PACAP−/−, respectively); ns = no significant difference to respective WT group, or between SOD1 and SOD1:PACAP−/−; # $p < 0.05$ between SOD1 and SOD1:PACAP−/−.

SOD1:PACAP−/− = 2.6 ± 1.5, data not displayed). A quantitative analysis of the parasympathetic vagal neurons (Fig. 4J) uncovered a substantial neuron loss in SOD1 mice compared to their respective WT group (WT = 134.6 ± 17.2 vs. SOD1 = 99.0 ± 7.7, $p < 0.0001$; and PACAP−/− = 139.9 ± 7.6 vs. SOD1:PACAP−/− = 83.2 ± 8.0, $p < 0.0001$; all N = 4, $n = 5$). More importantly, X motoneuron loss was more pronounced in SOD1:PACAP−/− mice compared to SOD1 mice (# $p = 0.013$).

In the IML, ChAT-immunoreactive neurons were found grouped into small clusters in WT and PACAP−/− (Figs. 4E + F). In both SOD1 groups, ChAT-immunoreactivity lined pathologic vacuoles that had displaced the IML neurons (Figs. 4G + H). Different to X, vacuoles were never found in IML soma. Quantification of IML motoneurons (Fig. 4K) revealed no significant loss at disease end-stage in SOD1 mice when compared to age-matched WT (WT = 4.12 ± 1.3 vs. SOD1 = 3.89 ± 1.4, p = ns). However, a significant reduction was detected when comparing PACAP−/− with SOD1:PACAP−/− mice (PACAP−/− = 4.67 ± 2.4 vs. SOD1:PACAP−/− = 3.12 ± 1.1, N = 4, $n = 30–40$, $p = 0.0007$), and also when comparing the two SOD1 genotypes (# $p = 0.015$).

Taken together, endogenous PACAP expression partially protected central visceromotor, but not somatomotor neurons against ALS-associated neurodegeneration, as what was reflected by an increased central visceromotor neuron loss in SOD1:PACAP−/− mice.

PACAP-deficiency prolongs survival and improves tongue motor function in SOD1 mice

Given the neuroprotective and live extending effects of PACAP shown in mouse models of e.g. Alzheimer's and Parkinson's diseases, trauma and stroke, it was expected that disease progression in SOD1:PACAP−/− was exacerbated compared to SOD1 littermates. Gathering the survival of all SOD1 mice, with and without the presence of PACAP (Fig. 5A), revealed a mean life expectancy of 132 days for the SOD1 group, and of 139.5 days for the SOD1:PACAP−/− group (p = 0.0022). Thus, surprisingly, SOD1:PACAP−/− mice survived 7.5 days (equaling 5.5%) longer compared to their PACAP-expressing SOD1 littermates.

During clinical monitoring, all groups showed a comparable initial increase in body weight (Fig. 5B). While WT and PACAP−/− mice constantly gained weight over time, SOD1 and SOD1:PACAP−/− mice reached their maximum weight at around P100, and started to gradually lose weight thereafter. No significant difference between the SOD1 and SOD1:PACAP−/− genotypes was observed at any time point before or after onset of body weight loss.

To investigate ALS-typical disturbances in motor performance corresponding to the investigated somatomotor neuron pool, the paw grip endurance (PaGE, corresponds to ventral horns of lumbar spinal cord) and licking tests (corresponds to XII) were performed. SOD1 and

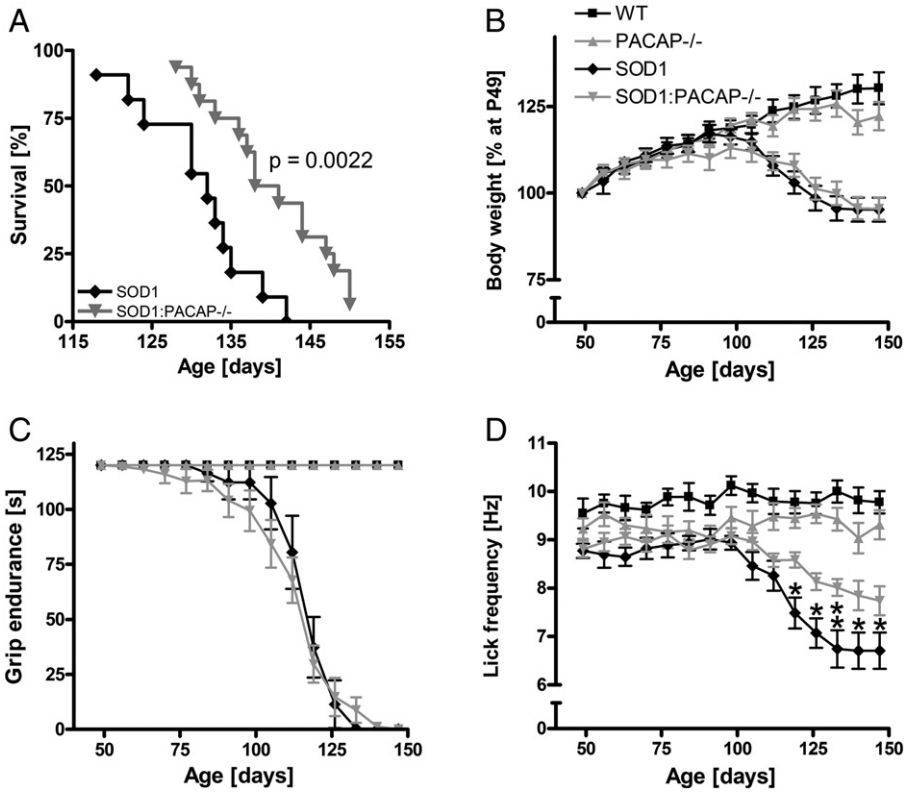

Fig. 5. (A) Survival analysis of SOD1 mice, revealing a significant extension of mean life expectancy of SOD1:PACAP–/– mice (139.5 days; $n = 16$) when compared to SOD1 mice (132.0 days; $n = 11$; $p = 0.0022$). Body weight (B) and motor functions (C + D) of all study groups (WT, $n = 18$; PACAP–/–, $n = 12$; SOD1, $n = 11$; and SOD1:PACAP–/–, $n = 16$) were monitored weekly starting at P49. Data were analyzed by two-way ANOVA with Bonferroni post hoc testing and results shown as means with SEM. Differences between SOD1 and SOD1:PACAP–/– mice at a given age are indicated by asterisks; $^{*}p < 0.05$; $^{**}p < 0.01$.

SOD1:PACAP−/− mice showed very similar declines in PaGE starting around P100 (Fig. 5C), without any differences between the two PACAP genotypes.

Analyzing tongue motor function (Fig. 5D), SOD1 mice in the pre-symptomatic phase (P49–84) showed a mean licking frequency of 8.8 ± 0.6 Hz and hence performed 1 Hz slower than their respective WT group with 9.8 ± 0.7 Hz. Although statistically not significant, this difference was noticeable compared to the two PACAP-deficient groups without broad discrepancies in initial licking frequency (P49–84: PACAP−/− 9.3 ± 0.8 Hz vs. SOD1:PACAP−/− 9.0 ± 0.7 Hz). Most noticeable, the SOD1:PACAP−/− mice showed a significant better tongue motor performance than the SOD1 group during the late symptomatic phase (P119-end), visible as a difference in curve steepness.

Altered microglia morphology is a characteristic of PACAP-deficient SOD1 mice

Since PACAP also has immunomodulatory properties, and neuroinflammation in ALS has a strong impact on disease progression, we investigated if PACAP depletion altered the different inflammatory components, i.e. lymphocyte infiltration and astrocyte and microglial activation. Again, para-median brain stem sections and lumbar spinal cord of SOD1 and SOD1:PACAP−/− mice were compared to age-matched WT and PACAP−/− animals, respectively, this time at a pre-symptomatic disease stage (all genotypes: P60) and at disease end stage of SOD1 mice (control animals: P120). For quantification, four sections per animal and four animals per stage/age/genotype were immunostained with specific markers for lymphocytes, astrocytes and microglia, respectively.

Lymphocytes were labeled by CD3 staining and counted as single cells using an algorithm based on optical density with a specific threshold. In the early disease state (P60), lymphocyte numbers were similar for all four study groups, both in brain stem and lumbar spinal cord (pre-symptomatic/P60 brain stem: WT = 2.8 ± 1.8 vs. SOD1 = 3.8 ± 1.4 vs. PACAP−/− = 3.4 ± 1.1 vs. SOD1:PACAP−/− = 5.8 ± 2.7, all p = ns; pre-symptomatic/P60 spinal cord: WT = 0.6 ± 0.6 vs. SOD1 = 1.3 ± 1.5 vs. PACAP−/− = 0.6 ± 0.6 vs. SOD1:PACAP−/− = 1.6 ± 1.5, all p = ns, data not displayed). Whereas lymphocyte numbers did not change in WT and PACAP−/− mice until P120, both SOD1 and SOD1:PACAP−/− showed a distinct and significant increase in cell number compared to their controls, without significant differences between the two PACAP genotypes (end-stage/P120 brain stem: SOD1 = 22.7 ± 9.9 vs. SOD1:PACAP−/− = 14.6 ± 5.4, p = ns; end-stage/P120 spinal cord: SOD1 = 4.0 ± 3.3 vs. SOD1:PACAP−/− = 3.4 ± 1.8, p = ns, data not displayed).

Astrocyte activation was quantified by determining the relative portion of GFAP immunoreactive area in para-median sections from pontine brain stem and in the ventral horn of lumbar spinal cord. In brain stem, all four genotypes showed about 15% GFAP positive area at P60, that doubled until disease end stage in SOD1 transgenic mice without difference between PACAP+/+ and PACAP−/− animals (SOD1 =31.7 ± 1.7% vs. SOD1:PACAP−/− = 29.0 ± 5.2%, p = ns). In accordance with previous observations (Ringer et al., 2009), an increase in the area covered by GFAP-positive astrocytes in lumbar spinal cord already occurred in the early disease state (pre-symptomatic/P60: WT = 19.1 ± 3.0% vs. SOD1 = 38.0 ± 8.8%, $p < 0.01$; PACAP–/– =19.3 ± 3.3% vs. SOD1:PACAP–/– = 37.6 ± 13.7%, $p < 0.001$, data not displayed). SOD1 and SOD1:PACAP–/– mice differed neither in early, nor in late disease stages, even after an additional strong increase of GFAP positive area to more than 50% until end-stage (SOD1 = 64.2 ±11.6% vs. SOD1:PACAP–/– = 66.5 ± 7.8%, p = ns, data not displayed).

Microglia were labeled by Iba1 staining and quantified, like astrocytes, as immunoreactive area. In the pre-symptomatic phase at P60, the proportion of microglia was similar in all four study groups, both in brain stem (WT = 0.052 ± 0.001% vs. SOD1 = 0.094 ± 0.016%, p = ns; PACAP−/− = 0.057 ± 0.015% vs. SOD1:PACAP−/− = 0.097 ± 0.021%, p = ns; data not displayed) and spinal cord (WT = 0.338 ± 0.096% vs. SOD1 = 0,506 ± 0,138%, p = ns; PACAP−/− = 0.325 ± 0.105% vs. SOD1:PACAP−/− = 0.572 ± 0.101%, p = ns; data not displayed). At end-stage, SOD1 mice showed a significant increase in Iba1 reactive area, both in brain stem and spinal cord, that was largely decelerated in SOD1:PACAP−/− mice (end-stage brain stem: SOD1 = 4.031 ± 1.400% vs. SOD1:PACAP−/− = 1.613 ± 0.664%, $p < 0.001$; end-stage spinal cord: SOD1 = 2.463 ± 0.353% vs. SOD1:PACAP−/− = 0.747 ± 0.163%, $p < 0.001$, data not displayed).

Remarkably, a difference in microglia morphology was obvious in SOD1:PACAP−/− mice when compared to SOD1 mice. As shown here in Fig. 6, in low and high magnifications, brain stem microglia from P120 WT (Figs. 6A + B) and PACAP−/− mice (Figs. 6D + E) were moderate in number and without visible processes, and with rather ramified morphology in the cortex (Figs. 6C + F). At disease end-stage, brain stem microglia from SOD1 mice had mostly acquired a hypertrophic morphology (Figs. 6G–H), while those in the cortex were rather amoeboid (Fig. 6I). Conversely, SOD1:PACAP−/− mice at disease end-stage had mostly amoeboid microglia in brain stem (Figs. 6J + K), while the cortical microglia were still ramified (Fig. 6L).

Taken together, while lymphocyte infiltration and astrocyte activation were not altered by PACAP-deficiency, the transition from amoeboid to hypertrophic microglia morphology that is known to occur during ALS disease progression in SOD1 mice (Appel et al., 2010; Beers et al., 2008; Henkel et al., 2009), was absent in SOD1:PACAP−/− mice.

Discussion

In our study we provide a detailed chemical neuroanatomical examination of both the expression of PACAP and its receptors, and ALS associated histopathological changes in the cellular compartments of brain stem and spinal cord motor systems of SOD1(G93A) mice, and investigated the functional and cytological effects of a PACAP deficiency, both before and during ALS disease progression. We elucidated PACAP dependent differences in vulnerability between the parasympathetic and the sympathetic divisions of the visceromotor system, and two functionally opposing roles of the PACAP ligand-receptor system on neuroprotection and neuroinflammation, respectively.

Differences in autonomic nervous system pathology in SOD1 mice

Our histological analysis of the ANS revealed that the pre-ganglionic divisions of both the parasympathetic and sympathetic nervous systems were morphologically affected during ALS pathology in SOD1(G93A) mice, with disease model-characteristic vacuolization equally present in nuclei of both systems. Vacuoles have been assigned to cell bodies and neurites of affected neurons (Ringer et al., 2009), and are thought to represent swellings of mitochondrial membranes, most probably leading to metabolic disturbances (Dupuis et al., 2011). ANS neuron loss, however, was restricted to the pre-ganglionic parasympathetic part, i.e. the dorsal vagal nucleus. In contrast, neither sympathetic pre-ganglionic neurons in the thoracic spinal cord nor the post-ganglionic divisions of both the parasympathetic and the sympathetic systems were found to degenerate. Our analysis thus not only unraveled a selective vulnerability of parasympathetic pre-ganglionic neurons in this ALS mouse model, but also that neurons affected by the pathology not necessarily are prone to die. Since also some somatomotor neurons, e.g. those innervating the external eye muscles, superficially do not degenerate during ALS disease progression in mice and humans (Haenggeli and Kato, 2002; Okamoto et al., 1993), our results may be an important finding for future investigations concerning molecular and physiological differences between ALS-resistant and vulnerable (motor) neurons. In addition, the observed preservation of the peripheral aspect of the ANS is in line with the concept of ALS being a disease primarily of the central nervous system.

Autonomic dysfunctions on a mere subclinical level have been reported both in human ALS patients and in SOD1(G93A) mice, suggesting that ALS is a multi-system disorder rather than a pure somatomotor neuron disease (Baltadzhieva et al., 2005). In SOD1 mice, especially an increase in heart rate at rest and following stress was measured (Kandinov et al., 2011), as was blood pressure significantly elevated at age 10–11 weeks of age, followed by a gradual decrease until end-stage (Kandinov et al., 2012). Relating these functional impairments to our morphological data is suggestive of an imbalanced centrally driven autonomic tone, where sympathetic hyperreactivity in SOD1(G93A) mice may be due to central parasympathetic hypoactivity

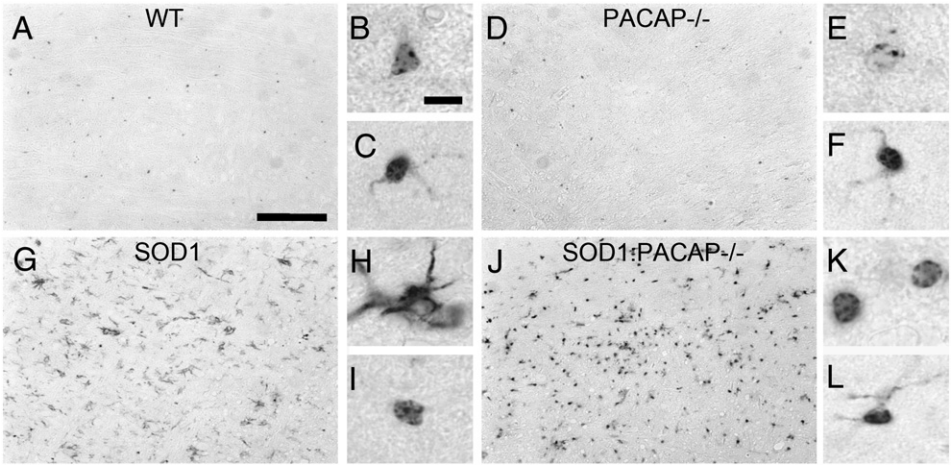

Fig. 6. Iba1 immunohistochemistry revealing different microglia morphology depending on SOD1 and PACAP genotypes and brain region, respectively. (A, D, G, J) Low magnifications of medullary brain stem. (B, E, H, K) High magnifications of single microglial cells located in the brain stem. (C, F, I, L) High magnifications of single microglial cells located in the motor cortex. In WT (A–C) and PACAP−/− (D–F) mice at P120, microglia showed ramified, resting morphologies, although the processes were hardly visible in the brain stem neuropil. In end-stage SOD1 mice (G–I), microglia in brain stem (G and H) were mostly hypertrophic to degenerating, resulting in weak Iba1 staining. In the cortex (I), microglia exhibited amoeboid morphology. In end-stage SOD1:PACAP−/− animals (J–L), microglia in brain stem (J and K) were strongly labeled by Iba1 and showed a predominantly amoeboid morphology. In the cortex (L), microglia with ramified morphology and clearly visible processes dominated. Scale bar in (A) equals 50 μm and applies to all low magnifications (A, D, G, J), and scale bar in (B) equals 5 μm and applies to all high magnifications (B, C, E, F, H, I, K, L).

caused by neuron loss. Data from individual ALS patients are rare and conflicting with evidence for both sympathetic and parasympathetic deterioration. In addition, clinically significant autonomic disturbances are infrequent in early ALS (Baltadzhieva et al., 2005), suggesting that their overall role for disease progression is of minor importance. However, since quality-of-life issues are of major interest in ALS palliative care, therapeutic targeting of the autonomic nervous system, e.g. to improve parasympathetic functions like salivation and thereby swallowing, deserves consideration.

Constitutive co-expression of PACAP with PAC1 as a mechanistic basis for autocrine cytoprotection of motor neurons in ALS

We show that pre-ganglionic visceromotor neurons, but not somatomotor neurons in WT and SOD1(G93A) mice constitutively express PACAP and at least one of its receptors, i.e. PAC1. The genetic depletion of PACAP in WT mice did neither result in somatomotor nor visceromotor degeneration, indicating that PACAP signaling is dispensable for the development and maintenance of these motoneuron pools. In SOD1(G93A) mice, however, absence of PACAP led to a further reduction in parasympathetic neuron numbers and, for the first time, to a loss of sympathetic neurons at disease end stage, while leaving somatomotor neuron degeneration unaffected. Although it remains puzzling why pre-ganglionic sympathetic neurons are more resistant to degenerate than are parasympathetic neurons, these results indicate that central ANS neurons are at least partially protected in a PACAP-dependent manner in the chronic neurodegenerative disease, ALS. Thus, our data support the general concept that constitutive co-expression of PACAP and PAC1 confers autocrine cytoprotection to chronically injured neurons. In this regard, endogenous PACAP has been assigned a crucial role in reducing neuronal damage caused by ischemia (Ohtaki et al., 2006) and pre-treatment with PACAP of rats challenged with 6-hydroxydopamine into the substantia nigra, a model of Parkinson's disease, reduced the loss of nigra neurons (Reglodi et al., 2004). In addition, increased neuronal vulnerability to various stressors in PACAP-deficient mice (reviewed by Reglodi et al., 2012) suggests that PACAP is protective independent of the kind of stress or injury or neuron type.

However, in spite of the observation that challenged somatomotor neurons in culture survive better in the presence of PACAP (Tomimatsu and Arakawa, 2008), no real evidence about functional neuroprotective effects of PACAP on somatomotor neurons in vivo exist. Although PACAP transcripts were found up-regulated/induced in axotomized facial motoneurons (Mesnard et al., 2011; Zhou et al., 1999), motoneuron survival was not significantly different in PACAP−/− vs. PACAP+/+ mice after facial nerve crush injury (Armstrong et al., 2008). Instead, axon regeneration was delayed in PACAP−/− mice, suggesting that PACAP supports the recovery of axotomized somatomotor neurons (Armstrong et al., 2008). In contrast to axotomy, PACAP was not found generally up-regulated or induced in somatomotor neurons in ALS in our study, indicating that PACAP response mechanisms to peripheral, acute injury like axotomy are not recapitulated in central, chronic neurodegeneration and thus are not directly comparable. Nevertheless, the finding of PAC1 and VPAC2 receptor expression in somatomotor neurons in this study suggests that although endogenous PACAP is neither induced nor cytoprotective in this neuron type in vivo in ALS, it may be neuroprotective or neurotrophic as a pharmacological agent or after a targeted induction, respectively. Therefore, it would be very interesting to study the effects of a targeted PACAP (over)expression in somatomotor neurons in SOD1(G93A) mice in further investigations, even more if an inducible model is used with PACAP expression induced after disease onset.

Life-prolonging effect of PACAP-deficiency: functional motor outcome matters

Although an additional visceromotor neuron loss was observed and hypoglossal somatomotor neuron loss was unchanged by PACAP-deficiency in SOD1(G93A) mice, SOD1:PACAP−/− mice lived significantly longer than their SOD1 littermates and licking performance is largely preserved until end-stage. Thus, a better functional state of the hypoglossal motor neurons and finally the tongue, that is not reflected by neuron number or morphology investigated in our study, may result in a better or extended fluid consumption time, resulting in a longer life span.

Prevention of a microglia phenotype switch in PACAP-deficient SOD1 mice

We show that a switch in microglia morphology from amoeboid to hypertrophic, which occurs during disease progression in SOD1(G93A) mice, is largely prevented in SOD1:PACAP−/− mice. This raises the possibility that PACAP may have functional relevance for the outcome of neuroinflammation in ALS. Neuroinflammation characterized by activation of glial cells has been found to drive disease progression during clinical stages in many types of neurodegeneration, including ALS (Philips and Robberecht, 2011). Although glial reactions were known to be associated with motoneuron degeneration for a long time, their direct relevance for ALS remained obscure until the seminal study by Clement and colleagues (Clement et al., 2003), and several studies thereafter (Beers et al., 2006; Boillée et al., 2006) proving that glial cells actively participate in motoneuron degeneration, at least in the SOD1(G93A) mouse model. Current assumptions emanate that in early disease stages neuroinflammation achieves a neuroprotective milieu slowing motor neuron degeneration, whereas in later stages the neuroinflammation becomes cytotoxic and forces disease progression (Kiernan et al., 2011; Philips and Robberecht, 2011).

In this scenario microglia switch from the alternative M2 phenotype, i.e. amoeboid morphology with secretion of interleukins (IL) 4 and 10, into the classical M1 phenotype marked by hypertrophy, antigen presentation and secretion of e.g. IL 6, tumor necrosis factor alpha (TNFα) and nitric oxide (NO) (Appel et al., 2010; Henkel et al., 2009). This concept, however, has been challenged by the process of microglia cytorrhexis, whereby microglia proceed to a dysfunctional state and lose their neuroprotective features (Streit, 2002; Streit and Xue, 2009). Accordingly, a therapeutic intervention that keeps glial functions on the neuroprotective and/or functional level, especially the microglia in the amoeboid M2 activation state, as did the PACAP-depletion in our study, could be a promising strategy in the treatment of ALS.

In the past, several studies have assigned PACAP an inhibitory role on the brains innate immunity, especially on microglial activation (Delgado et al., 2002; Kim et al., 2002), with these effects most likely mediated by VPAC1 (Delgado et al., 2003). Such anti-inflammatory actions of PACAP are thought to result in neuroprotection, because pathologic microglia activation is prevented. Microglia in the SOD1(G93A) mouse model of ALS, however, react in a different manner to certain stimuli (Weydt et al., 2004). It is thus possible that chronic suppression of microglial activation by PACAP during the early disease phase has detrimental effects on the final functional maturation of these cells and forces microglia to adopt a neurodestructive or dysfunctional "bad" activation state. Absence of PACAP, on the other hand, prolongs the time window in which "good" microglia are activated and can *functionally* protect motoneurons from degeneration.

A mechanistically similar, yet also unanticipated role has recently been discovered for the related neuropeptide VIP in experimental autoimmune encephalomyelitis. Here, endogenous VIP seems to have a permissive and pro-inflammatory function in the propagation of the inflammatory response during disease (Abad et al., 2010), indicating that members of this family of neuropeptides not only share some receptors (VPAC1 + 2), but are also functionally closely related.

Because both astrocytes and microglia express PAC-1 and VPAC1 (Grimaldi and Cavallaro, 1999; Kim et al., 2000) and maintain a permanent molecular crosstalk with each other (Moisse and Strong, 2006), we cannot exclude that the observed morphological phenotype of the

microglia in SOD1:PACAP−/− may be caused by indirect pathways, e.g. via changes in the cytokine profile of astrocytes.

Compared to autocrine neuroprotective actions of PACAP (see above), paracrine PACAP actions on glial cells are not per se beneficial for neurons in the SOD1(G93A) mouse model of ALS. Since cell morphology not necessary reflects a functional state, we cannot exclude that the amoeboid microglia in SOD1:PACAP−/− mice still exerts neurotoxic functions. But in contrast to the hypertrophic and probably dysfunctional microglia found in the brain stem of SOD1 mice, microglia from SOD1:PACAP−/− mice still look "healthy" and thus functional. In addition, microglia in the cortex of end-stage SOD1:PACAP−/− mice still showed a ramified morphology, indicating resting state. In contrast, microglia in the cortices of end-stage SOD1 mice were amoeboid. This provides strong evidence that the whole inflammatory process, i.e. both the propagation of the activation of microglia throughout the brain and the transition from neuroprotective to neurotoxic action, is slowed down by PACAP depletion. Given the possibility that central defects caused by inflammation of higher brain regions may contribute to disease progression and thereby influence survival, the impact of the PACAP depletion on the overall characteristics of microglia activation could be an explanation for the extended life time of SOD1:PACAP−/− mice. The full explication of the functional significance of the microglial morphological shift observed here on subsequent neuronal-microglial and astrocyte-microglial interactions remains a subject for further investigation. These will require specific pharmacological interventions in vivo directed at blockade of the microglial morphological shift which are not yet available, but might involve the use of PACAP receptor subtype-specific reagents that cross the blood–brain-barrier. Furthermore, cell type-specific inactivation of PACAP receptors through transgenic technology should provide additional valuable information.

Knowledge about how disease initiation on the one hand, and propagation on the other is affected by PACAP signaling will be valuable in further consideration of PACAP and related neuropeptides as potential therapeutics in progressive neurological disease.

Pharmacologic intervention in PACAP signaling as a new therapeutic perspective in ALS?

Recently a VPAC2 agonist, peptide histidine isoleucine, was found to up-regulate beneficial glutamate transporter activity in the corpus callosum of SOD1 rats (Goursaud et al., 2011). Our results further indicate that the VIP/PACAP receptor family plays distinct and significant roles in ALS. Therefore, specific PACAP receptor agonism and/or antagonism, respectively, could be promising strategies in ALS therapy, depending on the point of therapeutic intervention in the disease progress. More precisely, a specific PAC1 agonist (e.g. maxadilan (Lerner et al., 2007)) may be able to protect PAC1-expressing somatomotor neurons against degeneration during the ALS pathology, while a specific VPAC1 antagonist (e.g. PG97-269 (Ceraudo et al., 2008)) could maintain the neuroprotective M2 microglial phenotype and thereby decelerate disease progression. Of course, for the time being these approaches have to be tested in the SOD1(G93A) mouse model, before their therapeutic potential could be appraised for human ALS patients.

Supplementary data to this article can be found online at http://dx.doi.org/10.1016/j.nbd.2013.02.010.

References

Abad, C., Tan, Y.V., Lopez, R., Nobuta, H., Dong, H., Phan, P., Feng, J.M., Campagnoni, A.T., Waschek, J.A., 2010. Vasoactive intestinal peptide loss leads to impaired CNS parenchymal T-cell infiltration and resistance to experimental autoimmune encephalomyelitis. Proc. Natl. Acad. Sci. U. S. A. 107, 19555–19560.

Appel, S.H., Beers, D.R., Henkel, J.S., 2010. T cell-microglial dialogue in Parkinson's disease and amyotrophic lateral sclerosis: are we listening? Trends Immunol. 31, 7–17.

Arimura, A., Somogyvári-Vigh, A., Miyata, A., Mizuno, K., Coy, D.H., Kitada, C., 1991. Tissue distribution of PACAP as determined by RIA: highly abundant in the rat brain and testes. Endocrinology 129, 2787–2789.

Armstrong, B.D., Hu, Z., Abad, C., Yamamoto, M., Rodriguez, W.I., Cheng, J., Tam, J., Gomariz, R.P., Patterson, P.H., Waschek, J.A., 2003. Lymphocyte regulation of neuropeptide gene expression after neuronal injury. J. Neurosci. Res. 74, 240–247.

Armstrong, B.D., Abad, C., Chhith, S., Cheung-Lau, G., Hajji, O.E., Nobuta, H., Waschek, J.A., 2008. Impaired nerve regeneration and enhanced neuroinflammatory response in mice lacking pituitary adenylyl cyclase activating peptide. Neuroscience 151, 63–73.

Baltadzhieva, R., Gurevich, T., Korczyn, A.D., 2005. Autonomic impairment in amyotrophic lateral sclerosis. Curr. Opin. Neurol. 18, 487–493.

Beers, D.R., Henkel, J.S., Xiao, Q., Zhao, W., Wang, J., Yen, A.A., Siklos, L., McKercher, S.R., Appel, S.H., 2006. Wild-type microglia extend survival in PU.1 knockout mice with familial amyotrophic lateral sclerosis. Proc. Natl. Acad. Sci. U. S. A. 103, 16021–16026.

Beers, D.R., Henkel, J.S., Zhao, W., Wang, J., Appel, S.H., 2008. CD4+ T cells support glial neuroprotection, slow disease progression, and modify glial morphology in an animal model of inherited ALS. Proc. Natl. Acad. Sci. U. S. A. 105, 15558–15563.

Bogaert, E., d'Ydewalle, C., Van Den Bosch, L., 2010. Amyotrophic lateral sclerosis and excitotoxicity: from pathological mechanism to therapeutic target. CNS Neurol. Disord. Drug Targets 9, 297–304.

Boillée, S., Vande Velde, C., Cleveland, D.W., 2006. ALS: a disease of motor neurons and their nonneuronal neighbors. Neuron 52, 39–59.

Ceraudo, E., Tan, Y.V., Nicole, P., Couvineau, A., Laburthe, M., 2008. The N-terminal parts of VIP and antagonist PG97-269 physically interact with different regions of the human VPAC1 receptor. J. Mol. Neurosci. 36, 245–248.

Chen, W.H., Tzeng, S.F., 2005. Pituitary adenylate cyclase-activating polypeptide prevents cell death in the spinal cord with traumatic injury. Neurosci. Lett. 384, 117–121.

Chen, Y., Samal, B., Hamelink, C.R., Xiang, C.C., Chen, M., Vaudry, D., Brownstein, M.J., Hallenbeck, J.M., Eiden, L.E., 2006. Neuroprotection by endogenous and exogenous PACAP following stroke. Regul. Pept. 137, 4–19.

Clement, A.M., Nguyen, M.D., Roberts, E.A., Garcia, M.L., Boillée, S., Rule, M., McMahon, A.P., Doucette, W., Siwek, D., Ferrante, R.J., Brown, R.H., Julien, J.P., Goldstein, L.S., Cleveland, D.W., 2003. Wild-type nonneuronal cells extend survival of SOD1 mutant motor neurons in ALS mice. Science 302, 113–117.

Dejda, A., Sokołowska, P., Nowak, J.Z., 2005. Neuroprotective potential of three neuropeptides PACAP, VIP and PHI. Pharmacol. Rep. 57, 307–320.

Dejda, A., Seaborn, T., Bourgault, S., Touzani, O., Fournier, A., Vaudry, H., Vaudry, D., 2011. PACAP and a novel stable analog protect rat brain from ischemia: insight into the mechanisms of action. Peptides 32, 1207–1216.

Delgado, M., Jonakait, G.M., Ganea, D., 2002. Vasoactive intestinal peptide and pituitary adenylate cyclase-activating polypeptide inhibit chemokine production in activated microglia. Glia 39, 148–161.

Delgado, M., Leceta, J., Ganea, D., 2003. Vasoactive intestinal peptide and pituitary adenylate cyclase-activating polypeptide inhibit the production of inflammatory mediators by activated microglia. J. Leukoc. Biol. 73, 155–164.

Dickson, L., Finlayson, K., 2009. VPAC and PAC receptors: from ligands to function. Pharmacol. Ther. 121, 294–316.

Dupuis, L., Pradat, P.F., Ludolph, A.C., Loeffler, J.P., 2011. Energy metabolism in amyotrophic lateral sclerosis. Lancet Neurol. 10, 75–82.

Fahrenkrug, J., Hannibal, J., 2004. Neurotransmitters co-existing with VIP or PACAP. Peptides 25, 393–401.

Fuchs, A., Ringer, C., Bilkei-Gorzo, A., Weihe, E., Roeper, J., Schütz, B., 2010. Downregulation of the potassium chloride cotransporter KCC2 in vulnerable motoneurons in the SOD1-G93A mouse model of amyotrophic lateral sclerosis. J. Neuropathol. Exp. Neurol. 69, 1057–1070.

Goursaud, S., Focant, M.C., Berger, J.V., Nizet, Y., Maloteaux, J.M., Hermans, E., 2011. The VPAC2 agonist peptide histidine isoleucine (PHI) up-regulates glutamate transport in the corpus callosum of a rat model of amyotrophic lateral sclerosis (hSOD1G93A) by inhibiting caspase-3 mediated inactivation of GLT-1a. FASEB J. 25, 3674–3686.

Grimaldi, M., Cavallaro, S., 1999. Functional and molecular diversity of PACAP/VIP receptors in cortical neurons and type I astrocytes. Eur. J. Neurosci. 11, 2767–2772.

Gurney, M.E., Pu, H., Chiu, A.Y., Dal Canto, M.C., Polchow, C.Y., Alexander, D.D., Caliendo, J., Hentati, A., Kwon, Y.W., Deng, H.X., 1994. Motor neuron degeneration in mice that express a human Cu, Zn superoxide dismutase mutation. Science 264, 1772–1775.

Haenggeli, C., Kato, A.C., 2002. Differential vulnerability of cranial motoneurons in mouse models with motor neuron degeneration. Neurosci. Lett. 335, 39–43.

Hamelink, C., Tjurmina, O., Damadzic, R., Young, W.S., Weihe, E., Lee, H.W., Eiden, L.E., 2002. Pituitary adenylate cyclase-activating polypeptide is a sympathoadrenal neurotransmitter involved in catecholamine regulation and glucohomeostasis. Proc. Natl. Acad. Sci. U. S. A. 99, 461–466.

Hannibal, J., 2002. Pituitary adenylate cyclase-activating peptide in the rat central nervous system: an immunohistochemical and in situ hybridization study. J. Comp. Neurol. 453, 389–417.

Hayar, A., Bryant, J.L., Boughter, J.D., Heck, D.H., 2006. A low-cost solution to measure mouse licking in an electrophysiological setup with a standard analog-to-digital converter. J. Neurosci. Methods 153, 203–207.

Henkel, J.S., Beers, D.R., Zhao, W., Appel, S.H., 2009. Microglia in ALS: the good, the bad, and the resting. J. Neuroimmune Pharmacol. 4, 389–398.

Ilieva, H., Polymenidou, M., Cleveland, D.W., 2009. Non-cell autonomous toxicity in neurodegenerative disorders: ALS and beyond. J. Cell Biol. 187, 761–772.

Kandinov, B., Korczyn, A.D., Rabinowitz, R., Nefussy, B., Drory, V.E., 2011. Autonomic impairment in a transgenic mouse model of amyotrophic lateral sclerosis. Auton. Neurosci. 159, 84–89.

Kandinov, B., Drory, V.E., Tordjman, K., Korczyn, A.D., 2012. Blood pressure measurements in a transgenic SOD1-G93A mouse model of amyotrophic lateral sclerosis. Amyotroph. Lateral Scler. 13, 509–513.

Kiernan, M.C., Vucic, S., Cheah, B.C., Turner, M.R., Eisen, A., Hardiman, O., Burrell, J.R., Zoing, M.C., 2011. Amyotrophic lateral sclerosis. Lancet 377, 942–955.

Kim, W.K., Kan, Y., Ganea, D., Hart, R.P., Gozes, I., Jonakait, G.M., 2000. Vasoactive intestinal peptide and pituitary adenylyl cyclase-activating polypeptide inhibit tumor necrosis factor-alpha production in injured spinal cord and in activated microglia via a cAMP-dependent pathway. J. Neurosci. 20, 3622–3630.

Kim, W.K., Ganea, D., Jonakait, G.M., 2002. Inhibition of microglial CD40 expression by pituitary adenylate cyclase-activating polypeptide is mediated by interleukin-10. J. Neuroimmunol. 126, 16–24.

Kong, J., Xu, Z., 1998. Massive mitochondrial degeneration in motor neurons triggers the onset of amyotrophic lateral sclerosis in mice expressing a mutant SOD1. J. Neurosci. 18, 3241–3250.

Laburthe, M., Couvineau, A., Tan, V., 2007. Class II G protein-coupled receptors for VIP and PACAP: structure, models of activation and pharmacology. Peptides 28, 1631–1639.

Leceta, J., Gomariz, R.P., Martinez, C., Abad, C., Ganea, D., Delgado, M., 2000. Receptors and transcriptional factors involved in the anti-inflammatory activity of VIP and PACAP. Ann. N. Y. Acad. Sci. 921, 92–102.

Lerner, E.A., Iuga, A.O., Reddy, V.B., 2007. Maxadilan, a PAC1 receptor agonist from sand flies. Peptides 28, 1651–1654.

Llewellyn-Smith, I.J., 2009. Anatomy of synaptic circuits controlling the activity of sympathetic preganglionic neurons. J. Chem. Neuroanat. 38, 231–239.

Mertens, I., Husson, S.J., Janssen, T., Lindemans, M., Schoofs, L., 2007. PACAP and PDF signaling in the regulation of mammalian and insect circadian rhythms. Peptides 28, 1775–1783.

Mesnard, N.A., Sanders, V.M., Jones, K.J., 2011. Differential gene expression in the axotomized facial motor nucleus of presymptomatic SOD1 mice. J. Comp. Neurol. 519, 3488–3506.

Miyata, A., Arimura, A., Dahl, R.R., Minamino, N., Uehara, A., Jiang, L., Culler, M.D., Coy, D.H., 1989. Isolation of a novel 38 residue-hypothalamic polypeptide which stimulates adenylate cyclase in pituitary cells. Biochem. Biophys. Res. Commun. 164, 567–574.

Miyata, A., Jiang, L., Dahl, R.D., Kitada, C., Kubo, K., Fujino, M., Minamino, N., Arimura, A., 1990. Isolation of a neuropeptide corresponding to the N-terminal 27 residues of the pituitary adenylate cyclase activating polypeptide with 38 residues (PACAP38). Biochem. Biophys. Res. Commun. 170, 643–648.

Moisse, K., Strong, M.J., 2006. Innate immunity in amyotrophic lateral sclerosis. Biochim. Biophys. Acta 1762, 1083–1093.

Moller, K., Reimer, M., Ekblad, E., Hannibal, J., Fahrenkrug, J., Kanje, M., Sundler, F., 1997. The effects of axotomy and preganglionic denervation on the expression of pituitary adenylate cyclase activating peptide (PACAP), galanin and PACAP type 1 receptors in the rat superior cervical ganglion. Brain Res. 775, 166–182.

Ohtaki, H., Nakamachi, T., Dohi, K., Aizawa, Y., Takaki, A., Hodoyama, K., Yofu, S., Hashimoto, H., Shintani, N., Baba, A., Kopf, M., Iwakura, Y., Matsuda, K., Arimura, A., Shioda, S., 2006. Pituitary adenylate cyclase-activating polypeptide (PACAP) decreases ischemic neuronal cell death in association with IL-6. Proc. Natl. Acad. Sci. U. S. A. 103, 7488–7493.

Okamoto, K., Hirai, S., Amari, M., Iizuka, T., Watanabe, M., Murakami, N., Takatama, M., 1993. Oculomotor nuclear pathology in amyotrophic lateral sclerosis. Acta Neuropathol. 85, 458–462.

Papadeas, S.T., Kraig, S.E., O'Banion, C., Lepore, A.C., Maragakis, N.J., 2011. Astrocytes carrying the superoxide dismutase 1 (SOD1G93A) mutation induce wild-type motor neuron degeneration in vivo. Proc. Natl. Acad. Sci. U. S. A. 108, 17803–17808.

Pettersson, L.M., Heine, T., Verge, V.M., Sundler, F., Danielsen, N., 2004. PACAP mRNA is expressed in rat spinal cord neurons. J. Comp. Neurol. 471, 85–96.

Philips, T., Robberecht, W., 2011. Neuroinflammation in amyotrophic lateral sclerosis: role of glial activation in motor neuron disease. Lancet Neurol. 10, 253–263.

Rat, D., Schmitt, U., Tippmann, F., Dewachter, I., Theunis, C., Wieczerzak, E., Postina, R., van Leuven, F., Fahrenholz, F., Kojro, E., 2011. Neuropeptide pituitary adenylate cyclase-activating polypeptide (PACAP) slows down Alzheimer's disease-like pathology in amyloid precursor protein-transgenic mice. FASEB J. 25, 3208–3218.

Reglodi, D., Tamás, A., Somogyvári-Vigh, A., Szántó, Z., Kertes, E., Lénárd, L., Arimura, A., Lengvári, I., 2002. Effects of pretreatment with PACAP on the infarct size and functional outcome in rat permanent focal cerebral ischemia. Peptides 23, 2227–2234.

Reglodi, D., Tamás, A., Lubics, A., Szalontay, L., Lengvári, I., 2004. Morphological and functional effects of PACAP in 6-hydroxydopamine-induced lesion of the substantia nigra in rats. Regul. Pept. 123, 85–94.

Reglódi, D., Tamás, A., Lengvári, I., Toth, G., Szalontay, L., Lubics, A., 2006. Comparative study of the effects of PACAP in young, aging, and castrated males in a rat model of Parkinson's disease. Ann. N. Y. Acad. Sci. 1070, 518–524.

Reglodi, D., Kiss, P., Szabadfi, K., Atlasz, T., Gabriel, R., Horvath, G., Szakaly, P., Sandor, B., Lubics, A., Laszlo, E., Farkas, J., Matkovits, A., Brubel, R., Hashimoto, H., Ferencz, A., Vincze, A., Helyes, Z., Welke, L., Lakatos, A., Tamas, A., 2012. PACAP is an endogenous protective factor-insights from PACAP-deficient mice. J. Mol. Neurosci. 48, 617–622.

Ringer, C., Weihe, E., Schütz, B., 2009. Pre-symptomatic alterations in subcellular betaCGRP distribution in motor neurons precede astrogliosis in ALS mice. Neurobiol. Dis. 35, 286–295.

Ringer, C., Weihe, E., Schütz, B., 2012. Calcitonin gene-related peptide expression levels predict motor neuron vulnerability in the superoxide dismutase 1-G93A mouse model of amyotrophic lateral sclerosis. Neurobiol. Dis. 45, 547–554.

Rosen, D.R., Siddique, T., Patterson, D., Figlewicz, D.A., Sapp, P., Hentati, A., Donaldson, D., Goto, J., O'Regan, J.P., Deng, H.X., 1993. Mutations in Cu/Zn superoxide dismutase gene are associated with familial amyotrophic lateral sclerosis. Nature 362, 59–62.

Rothstein, J.D., 2009. Current hypotheses for the underlying biology of amyotrophic lateral sclerosis. Ann. Neurol. 65 (Suppl. 1), S3–S9.

Schütz, B., Reimann, J., Dumitrescu-Ozimek, L., Kappes-Horn, K., Landreth, G.E., Schürmann, B., Zimmer, A., Heneka, M.T., 2005. The oral antidiabetic pioglitazone protects from neurodegeneration and amyotrophic lateral sclerosis-like symptoms in superoxide dismutase-G93A transgenic mice. J. Neurosci. 25, 7805–7812.

Seaborn, T., Masmoudi-Kouli, O., Fournier, A., Vaudry, H., Vaudry, D., 2011. Protective effects of pituitary adenylate cyclase-activating polypeptide (PACAP) against apoptosis. Curr. Pharm. Des. 17, 204–214.

Shioda, S., Ohtaki, H., Nakamachi, T., Dohi, K., Watanabe, J., Nakajo, S., Arata, S., Kitamura, S., Okuda, H., Takenoya, F., Kitamura, Y., 2006. Pleiotropic functions of PACAP in the CNS: neuroprotection and neurodevelopment. Ann. N. Y. Acad. Sci. 1070, 550–560.

Streit, W.J., 2002. Microglia as neuroprotective, immunocompetent cells of the CNS. Glia 40, 133–139.

Streit, W.J., Xue, Q.S., 2009. Life and death of microglia. J. Neuroimmune Pharmacol. 4, 371–379.

Stroth, N., Liu, Y., Aguilera, G., Eiden, L.E., 2011. Pituitary adenylate cyclase-activating polypeptide controls stimulus-transcription coupling in the hypothalamic-pituitary–adrenal axis to mediate sustained hormone secretion during stress. J. Neuroendocrinol. 23, 944–955.

Tan, Y.V., Abad, C., Lopez, R., Dong, H., Liu, S., Lee, A., Gomariz, R.P., Leceta, J., Waschek, J.A., 2009. Pituitary adenylyl cyclase-activating polypeptide is an intrinsic regulator of Treg abundance and protects against experimental autoimmune encephalomyelitis. Proc. Natl. Acad. Sci. U. S. A. 106, 2012–2017.

Tomimatsu, N., Arakawa, Y., 2008. Survival-promoting activity of pituitary adenylate cyclase-activating polypeptide in the presence of phosphodiesterase inhibitors on rat motoneurons in culture: cAMP-protein kinase A-mediated survival. J. Neurochem. 107, 628–635.

Wang, G., Pan, J., Tan, Y.Y., Sun, X.K., Zhang, Y.F., Zhou, H.Y., Ren, R.J., Wang, X.J., Chen, S.D., 2008. Neuroprotective effects of PACAP27 in mice model of Parkinson's disease involved in the modulation of K(ATP) subunits and D2 receptors in the striatum. Neuropeptides 42, 267–276.

Weydt, P., Yuen, E.C., Ransom, B.R., Möller, T., 2004. Increased cytotoxic potential of microglia from ALS-transgenic mice. Glia 48, 179–182.

Zhang, Y., Malmberg, A.B., Sjölund, B., Yaksh, T.L., 1996. The effect of pituitary adenylate cyclase activating peptide (PACAP) on the nociceptive formalin test. Neurosci. Lett. 207, 187–190.

Zhou, X., Rodriguez, W.I., Casillas, R.A., Ma, V., Tam, J., Hu, Z., Lelievre, V., Chao, A., Waschek, J.A., 1999. Axotomy-induced changes in pituitary adenylate cyclase activating polypeptide (PACAP) and PACAP receptor gene expression in the adult rat facial motor nucleus. J. Neurosci. Res. 57, 953–961.